ANADOLU UNIVERSITY

PARAMETRIC STUDY OF ENERGY, EXERGY AND THERMOECONOMIC ANALYSES ON A VAPOR-COMPRESSION SYSTEM CASCADED WITH LIBR/WATER AND NH₃/WATER ABSORPTION CASCADE REFRIGERATION CYCLES

Ahmet Selim DALKILIÇ [1], [*], Ali ÇELEN [1], Alican ÇEBİ [1], Tolga TANER [2], Somchai WONGWISES [3]

[1] Department of Mechanical Engineering, Faculty of Mechanical Engineering, Yildiz Technical University, Istanbul, Turkey
[2] Department of Motor Vehicles and Transportation Technology, Vocational School of Technical Sciences, Aksaray University, Aksaray, Turkey
[3] Department of Mechanical Engineering, Faculty of Engineering, King Mongkut's University of Technology Thonburi, Bangkok, Thailand

ABSTRACT

Energy savings on cooling systems can be achieved using novel refrigeration cycles. To this end, vapor-compression/vapor-absorption cascade refrigeration systems may be a substitute for single-stage vapor-compression refrigeration systems. These cycles can use renewable energy sources such as geothermal and solar heat energy as well as waste heat from processes to provide cooling, and they also require less electrical energy than vapor-compression cycles with alternative refrigerants. In this study, vapor-compression and vapor-absorption cascade systems undergo second-law analysis for various cooling capacities. While lithium bromide-water and NH₃/H₂O are the working fluids in the vapor-absorption part, various refrigerants are used in the vapor-compression section. The refrigerants R134a and R600a as well as R410A and R407C are tested in the study. The effects on the coefficient of system performance (COP) of alterations in cooling capacity, superheating, and subcooling in the vapor-compression part; temperature in the generator and absorber; and degree of overlap in cascade condenser in the vapor-absorption part. The results were validated by values given in the literature. Improvements in the COPs of the vapor compression, vapor absorption, and cascade systems were obtained separately. According to the analyses, cascade systems' COP increases with generator and evaporator temperatures and also increase as condenser and absorber temperatures decrease. Moreover, the generator had the highest exergy-destruction rates, followed by the condenser and absorber, respectively. Electricity consumption and payback period were also determined by considering the various parameters of the study.

Keywords: Energy, Exergy, Refrigeration, COP, Cycle

1. INTRODUCTION

Extant research on energy and exergy analyses is summarized below.

Cimsit and Ozturk [1] designed a two-stage vapor-compression (VC) and absorption (VA) refrigeration cycle and performed a thermodynamic analysis for the cycle. Whereas NH₃/H₂O was preferred as a refrigerant in the VA division, NH₃ was preferred in the VC division. As a result, the performance of this two-stage refrigeration cycle was found to increase with generator and evaporator temperatures. Also, the maximum exergy loss occurred in the absorber and was tracked by the generator.

Solum and Heperkan [2] carried out the exergy analysis and found the effects of thermodynamic amount of a geothermal origin, dual-result absorption cycle working by means of the liquid pair, and LiBr/H₂O on cycle performance. A geothermal energy system was used as the heat source. The results of system analysis showed that the COP was greater than 1. Generally, this value is below 1 in the one-tier absorption cooling system. As a result, the exergy efficiency of the systems was examined.

*Corresponding Author: ahmet_selim_dalkilic@hotmail.com

Bouaziz et al. [3] investigated single- and double-stage absorption cycles using NH_3/H_2O. They showed various configurations and suggested a novel hybrid absorption/refrigeration cycle. Through analyzing energy and exergy, they decided that energy sources at reasonable temperatures such as solar and geothermal sources may be preferred for powering absorption refrigeration systems and that the COP had a satisfactory value around 0.28.

Cimsit et al. [4] analyzed the energy and exergy of VA cycles to conclude the best functioning pair. $LiBr/H_2O$ and NH_3/H_2O couples were studied using just R134a in a VC division. The results show that the first- and second-law thermodynamic studies were carried out for various operating temperatures of the system elements using just $LiBr/H_2O$ in the absorption section and using various refrigerants, namely NH_3, R134a, R410A, and CO_2 in the VC division.

Yakar et al. [5] investigated the energy and exergy of VA with $LiBr/H_2O$ and a mechanical compression refrigeration system with R134a at various evaporating temperatures. The outcomes show that the activity increased as the evaporation temperature increased. However, in a VA system, if the evaporation temperature increases, the exergy activity decreases, which is the opposite of a mechanical compression refrigeration system.

Kaynaklı and Yamankaradeniz [6] compared NH_3/H_2O and $LiBr/H_2O$ in a one-period VA cycle. The given thermodynamic quality of liquid and cycle success were examined at many different generator, condenser, evaporator, and absorber degrees. In general, the performance of the system using liquid $LiBr/H_2O$ was better than the system using liquid NH_3/H_2O.

Öcal and Pıhtılı [7] performed first- and second-law analyses on single-stage and multi-stage cooling systems, and they compared the refrigerants used in their VC system model. It was understood that R600a and R290 could be used as alternative refrigerants to R717 and R22 in terms of compressor outlet temperature, volumetric and second-law efficiency, and R410 could be used as an alternative to R22. In addition, the necessity of a multi-stage cooling system was demonstrated for operating conditions based on.
Selbas [8] investigated the effects of absorber temperature in absorption cooling systems working with $LiBr/H_2O$ and carried out thermoeconomic analysis on the absorber. As a result, absorber temperatures are selected to be designed variable of the system and optimum absorber areas with the corresponding temperatures were determined.

Seewald and Perez-Blanco [9] developed a model of the absorption process in a simple absorber using LiBr and H_2O as the working fluids. The model was applied to a particular absorber by a computer program. Using computer program simulations, they analyzed the effect of variance in several parameters (solution flow rate, coolant flow rate, number of sites, absorber vapor pressure) on absorber performance. Knowing that absorption performance is highly affected by absorber performance and predicting absorber performance are useful.

Solum et al. [10] measured the effect of thermodynamic measures of any two-stage absorption cycle organized by two liquids, $LiBr/H_2O$ on cycle success. The COP of the cycle was evaluated using different degrees and compressions of the cycle elements. The results showed that the degrees and compression in a two acting absorption refrigeration system requires extremely precise arrangements.

Yakut et al. [11] used LiBr fluid in an absorption system aimed at conditioning a meeting hall for 30 people. The climate system's operating conditions and cooling loads were calculated by month. The head load of the generator was obtained by using planar solar collectors. Consequently, the number of solar collectors needed to provide the heating load requirements was calculated.

Jain et al. [12] investigated the size and cost of a VC–VA cascaded refrigeration system for a water-chilling facility that used R410a and LiBr/H_2O as refrigerants in the compression and absorption divisions. The main objective of the optimization was to minimize the total annual cost of the system. The conclusion parameters were the temperatures of the evaporator, condenser, generator, absorber, and cascade condenser as well as the degree of overlap and efficiency of the solution heat exchanger. A second-law analysis was performed. The optimization outcomes revealed that the higher capital costs of the system were offset by the system's lower performance and operating costs.

Jain et al. [13] analyzed the performance of a VC–VA cascaded refrigeration system under fouled conditions. R22 and LiBr/H_2O were each evaluated as refrigerants in the compression and absorption sections. In the final analysis, the system was found to have lower electricity consumption than that of a vapor-compression system with equal cooling capacity.

Karakas et al. [14] performed a suitability analysis for each component in a system and arranged the consequences in a table. The LiBr/H_2O system was found to be more efficient, based on botü first and second thermodynamic law examinations at temperatures higher than 0 °C.

Some of the papers with thermoeconomic analyses are summarized below.

Jain et al. [15] performed first-law analysis of a VC and VA cascade system. Ammonia–water solution was evaluated as a refrigerant in VA division, and R407C was used in the vapor-compression division. It was determined that the COP of the vapor-compression division of the CS might be enhanced and the electricity consumption could be reduced. Furthermore, the COP of CS at high cooling capacity was not independent of the condenser's performance.

Tailor and Vipin [16] examined a refrigeration cycle in which a compression system at the reduced degree period and an absorption cycle at the superior degree cycle were cascaded to develop a refrigeration system at the superior degree. These systems were examined thermodynamically and were compared and crosschecked with each other using various liquids in the compression and absorption sections and the same operating conditions and parts at operating states that were exactly alike. This presented the most suitable middle degree at which the system showed higher COP for CS.

Kaynakli and Yamankaradeniz [17] investigated the effect of heat exchangers, which are used to recover heat energy in VA systems, on COP. A NH_3/H_2O solution was taken as an absorbent–refrigeration pair. They found that the most effective heat exchanger in terms of system performance was a solution heat exchanger and that the system performance increased as the generator and evaporator temperatures increased, but decreased as the condenser and absorber temperatures increased.

Mukhopadhyay and Chowdhury [18] made a theoretical modeling of solar-assisted cascade refrigeration system in cold storage. The system consists of electricity-driven VC system and solar-driven vapor-absorption refrigeration system. The VC system is connected in series with vapor-absorption refrigeration system. They analyzed and found out COP of the cascade refrigeration system is up to the maximum when COP of the conventional vapor-compression refrigeration system is minimal.

Sözen and Ataer [19] examined NH_3/H_2O working with heat exchangers located in the VA system, finding that the system affected performance. For their research, the authors conducted first-law and second-law thermodynamic analysis for three different situations. These three situations are two heat exchangers, only the refrigerant heat exchanger, only the heat exchanger mixture. The system composed of condenser, evaporator, separators, pumps, expansion valves, cooling and the mixture heat exchangers. COP, ECOP and movement rate (f) were calculated for different evaporator, condenser and separators, with the effects on heat exchanger system performance examined.

Talbi and Agnew [20] examined a thermodynamic system in the VA cycle in terms of a large quantity of warmth to the habitat. The warmth developed exceeded that of the surrounding environment's temperature, which led to a crucial, irreparable loss in the cycle components. The authors examined exergy analysis using LiBr/H$_2$O fluid pairs. Numerical consequences were arranged as a table. As a result, COP of system was calculated.

Jain et al. [21] analyzed the performance of a VC-VA cascaded refrigeration system under fouled conditions. R22 and LiBr/H$_2$O were used as refrigerants in the compression and the absorption division, correspondingly. In the final analysis, it was found that electricity consumption was lower than that of vapor compression system for the same cooling capacity.

In this study, first- and second-law analyses of compression-absorption CS has been investigated using various refrigerants in VC subdivision and LiBr/H$_2$O and NH$_3$/H$_2$O fluid pairs in the VA subdivision. In the VC division, refrigerants, such as R134a, R407c, R410a and R600a, were considered under the same conditions. In the VA division, LiBr/H$_2$O and NH$_3$/H$_2$O fluid pairs were only used to compare the system's performance according to the type of refrigerants in VC division.

2. THERMODYNAMIC ENERGY BALANCES OF THE CASCADE CYCLE AND ITS DESCRIPTION

The base compression-absorption cascade refrigeration cycle with five total cycles was investigated in this study; please see Figure 1. The cycle investigated in this study is very similar to the classical cascade cycle, which is a form of absorption and VC cycles. The VC section of the system is very similar to a basic cooling cycle. However, in the absorption section of the cycle, a generator, a heat exchanger, a pump, an expansion valve and an absorber are preferred over a compressor to provide energy efficiency. In the VC section, different refrigerants were used, and LiBr/H$_2$O was used in the absorption section of the system. In the VC section, R134a, R407c, R410a, R600a were separately employed to compare the performance of different refrigerants. Ln P-h and T-s diagrams of the single-effect VC-VA cascade refrigeration cycle can be seen in Figures 2 and 3, respectively.

In the system, the weak LiBr solution is drawn by a pump from the absorber and then passes through a heat exchanger. Then, the high-pressured solution leaves the exchanger and passes through the generator. Next, the water in the solution passes through the condenser, resulting in a highly concentrated LiBr solution that leaves the generator and moves through the heat exchanger. Later, the low-pressured solution passes through a valve. Finally, the solution goes to the absorber. In the absorption section of the system, a heat exchanger is used to recover energy from the strong solution to the weak solution. After VA division of the system, the cooling water enters the condenser and leaves the condenser as a saturated liquid, providing ambient heat. Then, water leaves through the expansion valve with a pressure drop, and it is directed to the evaporator with the same enthalpy. In the evaporator, the heat rejected in the condenser of the VC division is absorbed and evaporates. In the end, this steam passes through the absorber and is absorbed by a hot solution in this section. However, in the vapor-compression section, the refrigerant pressure is increased by the compressor. After that, superheated and high-pressured refrigerant is sent to the condenser and leaves the condenser as a saturated liquid. Then, it passes through the expansion valve at a lower pressure. Finally, the refrigerant moves through the evaporator and leaves as saturated steam.

There are some thermodynamic assumptions needed to conduct thermodynamic analysis of the cycles:

1. The whole system is operated in steady-state.
2. The refrigerants' states at the exit of the evaporator and condenser are saturated vapor and saturated liquid, respectively.

3. The weak refrigerant solution at the exit of the absorber and strong solution at the exit of the generator are saturated.

4. Pressure losses in the system components are neglected.

5. In the absorption section of the system, pump work input is negligible.

6. The isentropic efficiency of the compressor is 0.80, and its electric efficiency is 0.90.

7. The environment temperature and pressure are assumed to be 298K and 101.325 kPa, respectively, for second-law analysis.

8. Changes in the kinetic and potential energies are negligible.
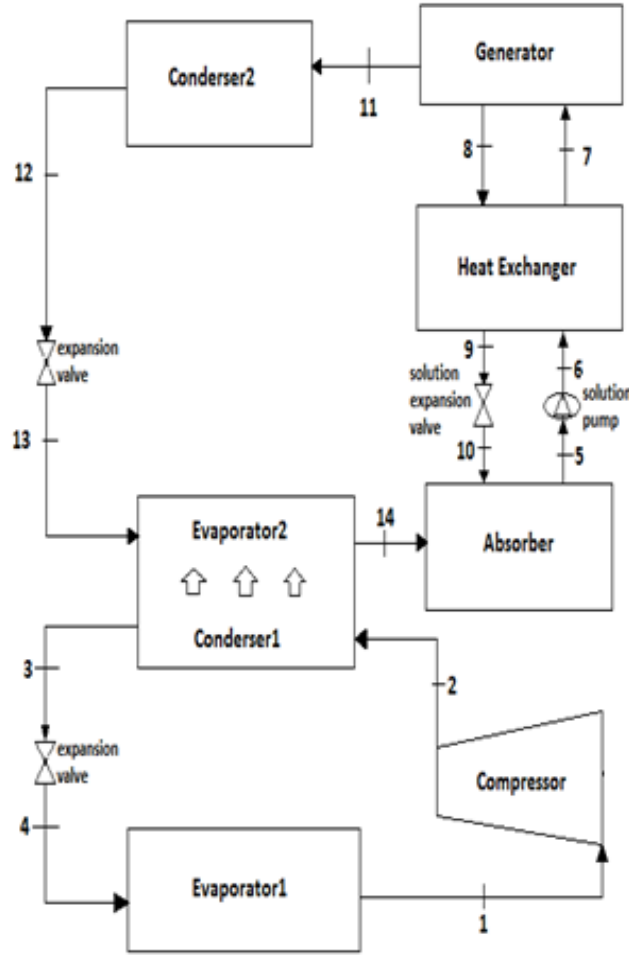
Figure 1. Schematic view of the single-effect compression-absorption cascade refrigeration cycle

The lnP-h and T-s diagrams of the single-effect compression-absorption CS are shown below.

The heat capacity of the components in the VC division of the cascade cycle can be obtained from the following equations:

$$W_{comp} = \dot{m}_1(h_2 - h_1) \tag{1}$$

$$\dot{Q}_{con1} = \dot{m}_3(h_3 - h_2) \tag{2}$$

$$\dot{Q}_{evap1} = \dot{m}_1(h_1 - h_4) \tag{3}$$

The heat capacity and the circulation ratio of the components in the VA division of the CS can be obtained from the following equations:

$$\dot{Q}_{con2} = \dot{m}_{11}(h_{11} - h_{12}) \tag{4}$$

$$\dot{Q}_{abs} = \dot{m}_{10}h_{10} + \dot{m}_{14}h_{14} - \dot{m}_{5}h_{5} \tag{5}$$

$$\dot{Q}_{gen} = \dot{m}_{11}h_{11} + \dot{m}_{8}h_{8} - \dot{m}_{7}h_{7} \tag{6}$$

$$\dot{Q}_{evap2} = \dot{m}_{13}(h_{14} - h_{13}) \tag{7}$$

Furthermore, COP for the overall CS is defined as:

$$COP_{cyclegen} = \frac{\dot{Q}_{evap1}}{\dot{Q}_{gen} + \dot{W}_{comp}} \tag{8}$$
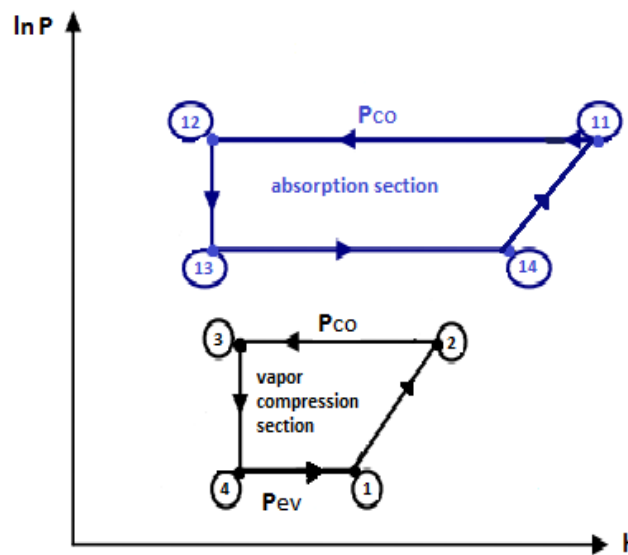
Figure 2. lnP-h diagram of the single-effect compression-absorption cascade refrigeration cycle
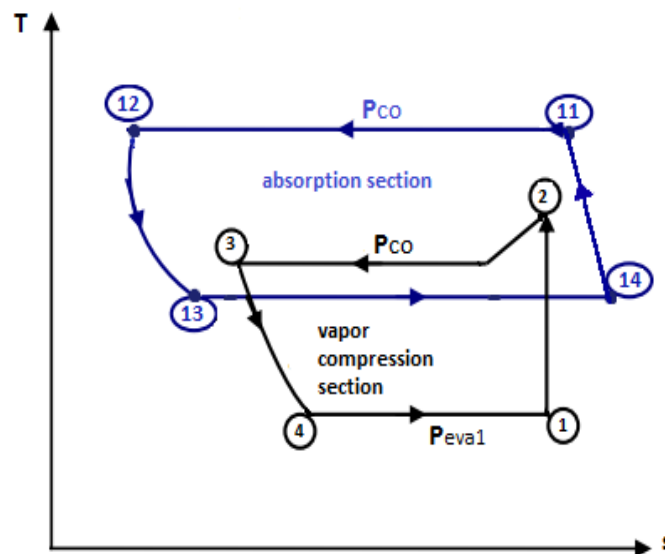
Figure 3. T-s diagram of the single-effect compression-absorption cascade refrigeration cycle

The annual net saving is determined as follows:

$$NS = \frac{PC_{VC}}{PC_{CS}} \tag{9}$$

In the equation above PC_{VC} and PC_{CS} mean the power consumption of VC and CS cycle respectively. The ratio of these two values gives the net saving ratio (NS) since it implies how many times greater the power cost of the considered systems. Thermodynamic properties at various points of the VC-VA system using R134a-NH₃/H₂O as working fluid are represented in Table 1.

3. SECOND-LAW ANALYSIS OF THE CASCADE REFRIGERATION CYCLE

To apply second-law analysis to CS, exergy analysis is conducted. Exergy is the maximum theoretical work during a process that brings the system into equilibrium with the environment. Specifically, exergy is also known as available useful work.

The exergy balance equation for a control volume is as follows:

$$\sum \dot{m}_i e_i - \sum \dot{m}_a e_a + \sum \dot{Q}(1 - \frac{T_0}{T}) - \sum W - E_D = 0 \tag{10}$$

In this equation, the first two terms show the sum of the exergy input and output according to the time rate. The third term is the exergy transfer rate with heat transfer. The fourth term is the energy transfer by mechanical work according to the time rate. The fifth term represents the time rate of exergy destruction due to irreversibility in the control volume.

The specific flow exergy can be evaluated using the equation below in case of the neglect of the changes in kinetic and potential energies.

$$e = (h - h_0) - T_0(s - s_0) \tag{11}$$

Furthermore, in a system, there are some points that may cause exergy destruction, such as friction losses, heat transfer and unrestricted expansion. In addition, mixture losses in the absorber and generator may also cause exergy loss in absorption systems. The rate of exergy destruction in each component of

Table 1. Thermodynamic values of VC-VA cascade refrigeration cycle as a function of R134a refrigerant in the VC division of the cycle

Fluid	Point	T (K)	h (kj/kg)	m (kg/s)	x (NH₃ %)
R134a	1	243	392.57	0.2973	-
	2	343	415.45	0.2973	-
	3	273	224.45	0.2973	-
	4	243	224.45	0.2973	-
NH₃/H₂O	5	303	-109.7	0.248	0.51
	6	303	-109.7	0.248	0.51
	7	331	21.5	0.248	0.51
	8	363	176.7	0.196	0.38
	9	327	11.3	0.196	0.38
	10	327	11.3	0.196	0.38
NH₃	11	363	1635	0.052	-
	12	303	322.9	0.052	-
	13	273	322.9	0.052	-
	14	273	1443.5	0.052	-

a VC-VA cascade refrigeration cycle can be determined from:

$$E_{Dgen} = \dot{m}_7 e_7 - \dot{m}_{11} e_{11} - \dot{m}_8 e_8 + \dot{Q}_{gen}(1 - \frac{T_0}{T}) \tag{12}$$

$$E_{Dabs} = \dot{m}_{10} e_{10} - \dot{m}_{14} e_{14} - \dot{m}_5 e_5 + \dot{Q}_{abs}(1 - \frac{T_0}{T_{abs}}) \tag{13}$$

$$E_{Dcon2} = \dot{m}_{11} e_{11} - \dot{m}_{12} e_{12} - \dot{Q}_{con}(1 - \frac{T_0}{T_{con2}}) \tag{14}$$

$$E_{Dshe} = \dot{m}_6 (e_6 - e_7) + \dot{m}_8 (e_8 - e_9) \tag{15}$$

$$E_{Devap2} = \dot{m}_2 (e_2 - e_3) + \dot{m}_{13}(e_{13} - e_{14}) \tag{16}$$

$$E_{Devap1} = \dot{m}_4 e_4 - \dot{m}_1 e_1 - \dot{Q}_{evap1}(1 - \frac{T_0}{T_{evap1}}) \tag{17}$$

$$E_{Dcomp} = \dot{m}_1 e_1 - \dot{m}_2 e_2 + \dot{W}_{comp} \tag{18}$$

$$E_{Dsev} = \dot{m}_9 e_9 - \dot{m}_{10} e_{10} \tag{19}$$

$$E_{Drev1} = \dot{m}_{12} e_{12} - \dot{m}_{13} e_{13} \tag{20}$$

$$E_{Drev2} = \dot{m}_3 e_3 - \dot{m}_4 e_4 \tag{21}$$

The total exergy destruction rate in the components of CS is determined from:

$$E_{Dt} = \sum_{i=1}^{n} \dot{E}_i \tag{22}$$

To determine the exergetic efficiency and performance of the system in terms of the second law of thermodynamics, ECOP value is calculated, and it is defined as the ratio between the useful exergy obtained from a system and that supplied to the system. Additionally, the useful exergy obtained from a system can be described as heat exchange between evaporator and the environment; the exergy supplied to the system can also be described as heat exchange between the generator and compressor's heat source and work. Thus, exergetic efficiency is expressed by:

$$E_{cop} = \frac{Q_{evap1}(1 - \dfrac{T_0}{T_{evap1}})}{Q_{gen}(1 - \dfrac{T_0}{T_{gen}}) + \dot{W}_{comp}} \tag{23}$$

4. RESULTS AND DISCUSSION

The following results are obtained for the energy and exergy analyses.

COP and ECOP are calculated by means of Eq. (8) and (22), respectively. The results for COP and ECOP can be seen in Table 2 for different refrigerants and the LiBr/H₂O pair. It should be noted that

the evaporation, generator, condenser 1 and condenser 2 temperatures were assumed as 263 K, 356 K, 291 K and 313 K, respectively. The COP results show that R600a is the most efficient refrigerant with a COP value of 0.772,. The ECOP results show that R600a is the most efficient refrigerant with an ECOP value of 0.423, followed by R410a, R407c and R134a in descending order of efficiency.

The total exergy destruction rates of the cycles are shown in Table 3. The exergy destruction results are obtained using numerous equations, specifically Eq. (9) to Eq. (21). Table 3 reveals that using R600a refrigerant in the VC division of the cycle causes more exergy destruction, with approximately 7.64 kW, followed by R134a, R407c, and R410a in descending order of efficiency. Furthermore, using R410a in the VC division of the cascade cycle causes the least exergy destruction, approximately 3.91 kW.

Figures 4 and 5 show the COP and ECOP values of the cascade refrigeration cycle for different evaporator pressures of the VC division of CS, respectively. Although evaporator pressure in the VC section increases, the COP and ECOP increase as well. The most significant increase in COP and ECOP is observed when R600a is the refrigerant in VC division of the cycle. With the usage of R600a in the VC division of the cycle, the COP and ECOP reach 1.4 and 0.95, respectively. In addition, using other refrigerants in the VC division causes slight increases in COP and ECOP.

Figure 6 shows the variation of evaporator1 capacity with evaporator pressure. The evaporator1 capacity calculated by Eq. (3) increased with increasing evaporator pressure. These results show that evaporator1 capacities of the cycles working with LiBr/H_2O-R600a has the highest evaporator capacity. It should be noted that evaporator1 capacities are determined as 76.09 kW and 37.62 kW at 1.5 bar for related cycles. Figure 7 represents the exergy destruction rate with evaporator temperature. The exergy destruction rate calculated by Eq. (21) decreases with increasing evaporator temperature. These results show that the cycle working with LiBr/H_2O-R600a has the highest exergy destruction rate in the range of 249 K and 263 K, whereas the cycle working with LiBr/H_2O- R410a and LiBr/H_2O-R407c have the lowest exergy destruction rates, in the range of 263 K and 277 K. However, LiBr/H_2O-R600a is observed to have the least exergy destruction rate by increasing temperature because of the high enthalpy changes.

Figures 8 and 9 demonstrate the variations of COP and ECOP with generator temperature, respectively. It can be seen from Figure 8 that COP decreases as the generator temperature of CS increases. The highest COP value obtained is 1.04 at 349 K in the generator of the absorption section of the cycle.

Table 2. Performance of CS for different refrigerants in the vapor-compression section for T_{evap1}=263 K, T_{gen}=356 K, T_{con1}=291 K, T_{con2}=313 K

Refrigerant- LiBr/H_2O	COP	ECOP
R134a - LiBr/H_2O	0.624	0.333
R407c - LiBr/H_2O	0.682	0.381
R410a - LiBr/H_2O	0.723	0.421
R600a - LiBr/H_2O	0.772	0.423

Table 3. Total exergy destruction rates of the CS for different refrigerants in the VC division for T_{evap1}=263 K, T_{gen}=356 K, T_{con1}=291 K, T_{con2}=313 K

| Refrigerant- LiBr/H_2O	Total Exergy Destruction
R134a - LiBr/H_2O	7.075
R407c - LiBr/H_2O	5.296
R410a - LiBr/H_2O	3.918
R600a - LiBr/H_2O	7.649
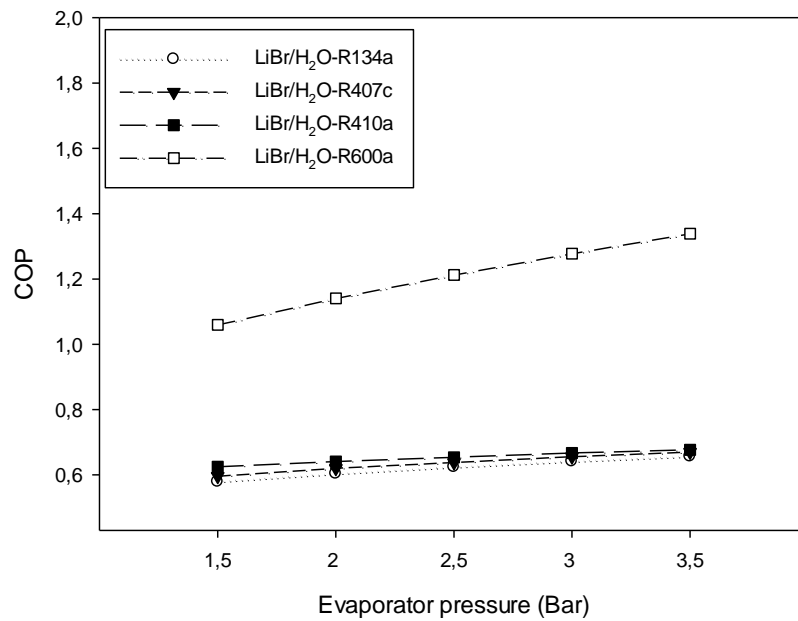
Figure 4. COP at different evaporator1 pressures for T_{con1}= 291 K, T_{con2}= 313 K, T_{gen}= 363 K
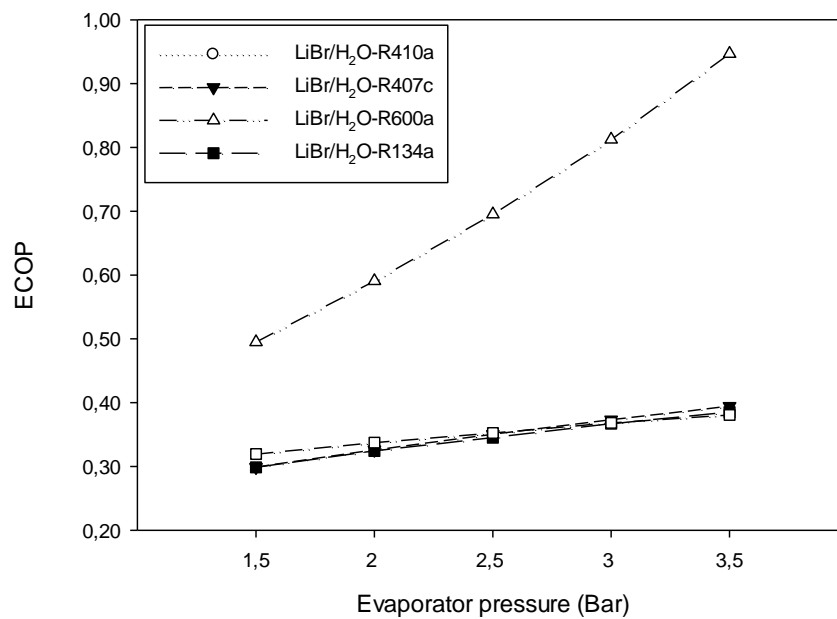
Figure 5. ECOP at different evaporator1 pressures for T_{con1}= 291 K, T_{con2}= 313 K, T_{gen}= 363 K
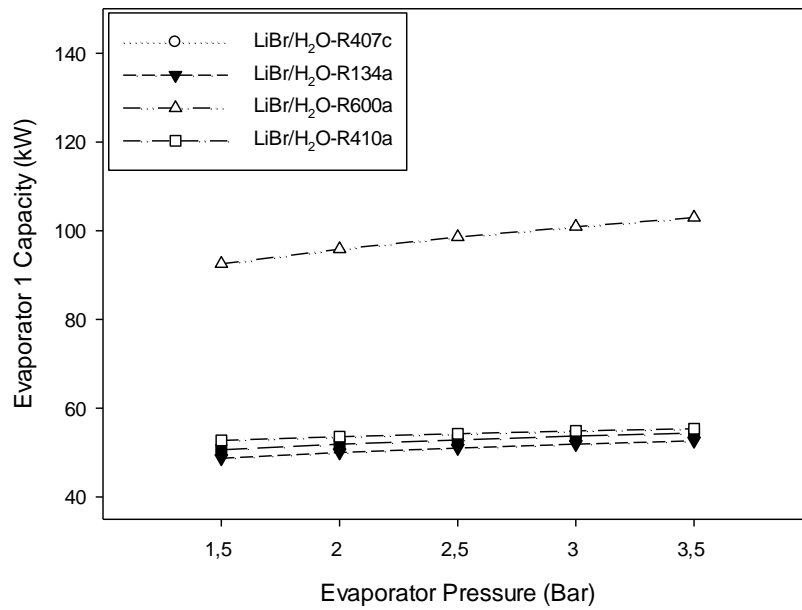
Figure 6. The variation of evaporator1 capacity with different evaporator1 pressures for T_{con1}= 291 K, T_{con2}= 313 K, T_{gen}= 363 K
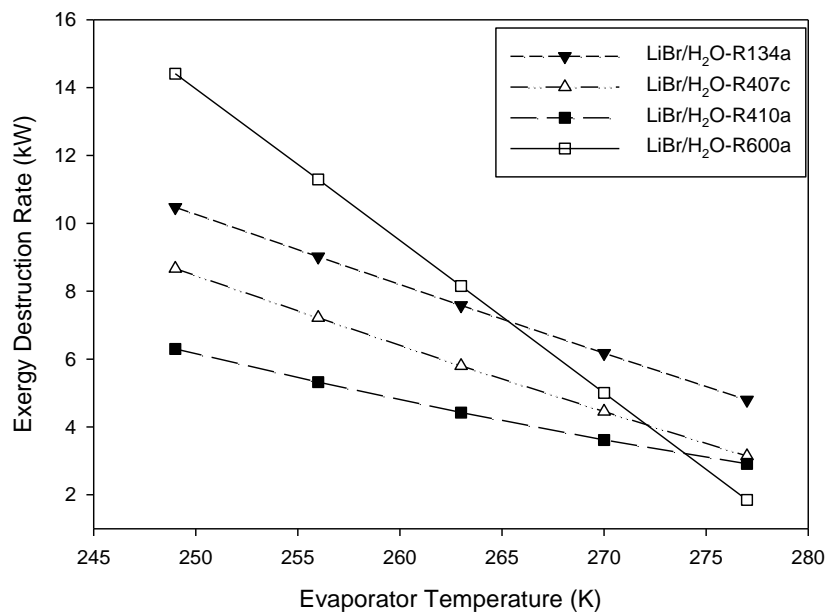

Figure 7. Exergy destruction rates at different evaporator1 temperatures for T_{con1}= 291 K, T_{con2}= 313 K, T_{gen}= 363 K

Moreover, R134a has the poorest performance with 0.60 as shown in Figure 8.

In Figure 9, it is clearly seen that ECOP slightly decreases as generator temperature increases. The main reason for ECOP decrease is the irreversibility factor. Irreversibility increases as generator temperature increases because of the external thermal energy needed by the system. There is also irreversibility in the system's evaporation process. As expected, the ECOP value of LiBr/H$_2$O-R600a is estimated to be 0.40 at 377 K.

Figure 10 shows the variation of generator capacity for different generator temperatures. It should be noted that generator capacity is estimated by means of Eq. (6). As seen in the figure, it increases as generator temperature increases, with a maximum value of 81.3 kW.
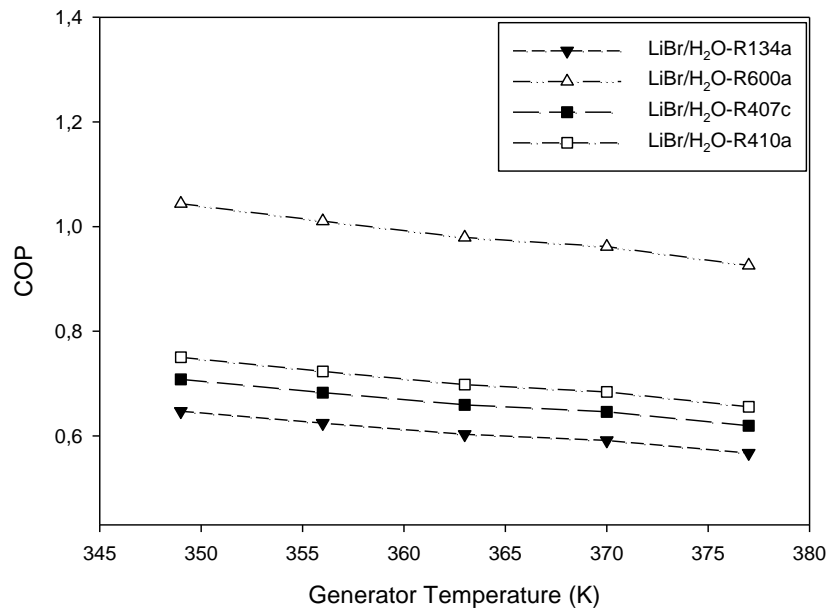

Figure 8. COP for different generator temperatures in various refrigerants for T_{con1}= 291 K, T_{con2}= 313 K, T_{evap1}= 263 K
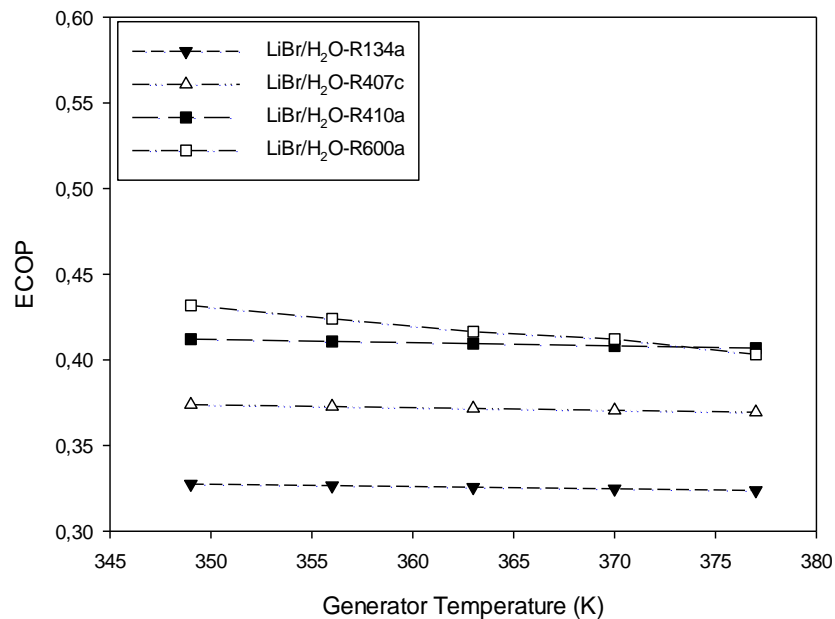

Figure 9. E_{COP} for different generator temperatures for T_{con1}= 291 K, T_{con2}= 313 K, T_{evap1}= 263 K

Figure 11 illustrates the exergy destruction rates of the system in various refrigerants in the VC division of the cycle. The exergy destruction rates increase as generator temperature increases. Furthermore, using R600a in the VC division of the cycle causes the greatest amount of exergy destruction, with a rate of 9.09 kW. However, pressure for Tcon1= 291 K, Tevap1= 263 K, Tgen= 363 K using R410 in VC division of the cycle causes the lowest exergy destruction rate. As a result, the highest ECOP is observed when R410 is used as a refrigerant in the VC division of CS.
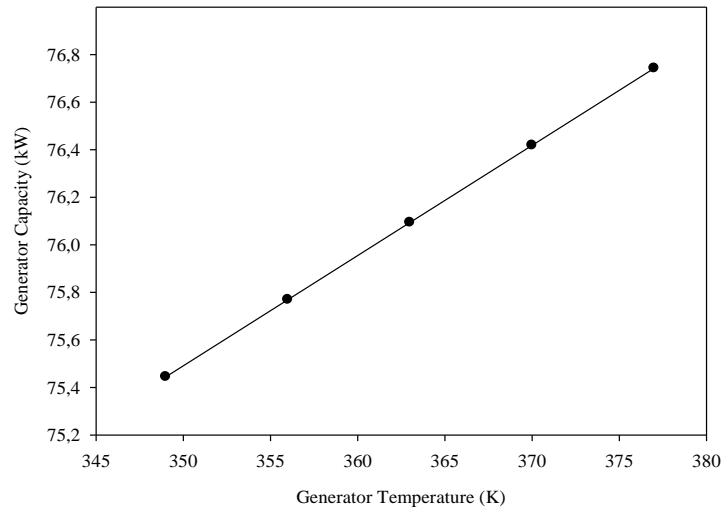
Figure 10. The variation of generator capacity for different temperatures in generator for T_{con1}= 291 K, T_{con2}= 313 K, T_{evap1}= 263 K
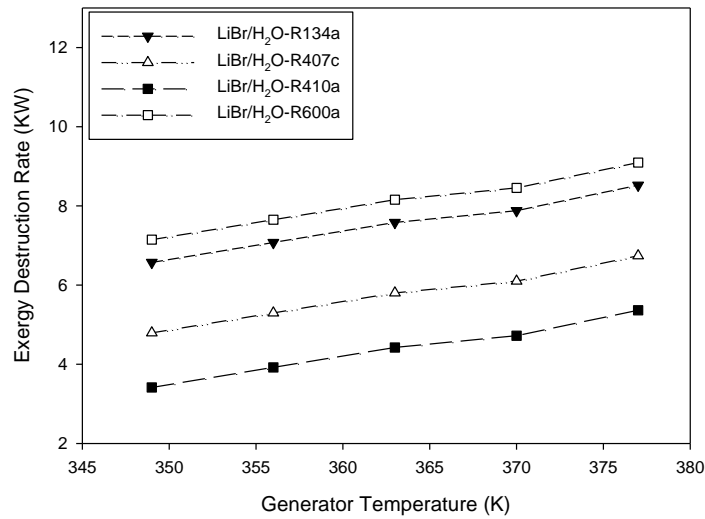

Figure 11. Exergy destruction rates for different generator temperatures for T_{con1}= 291 K, T_{con2}= 313 K, T_{evap1}= 263 K
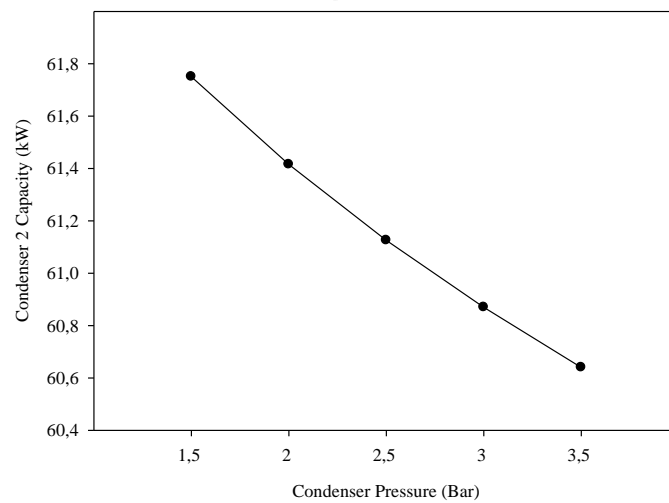

Figure 12. Condenser 2 capacity according to the changes in condenser pressure
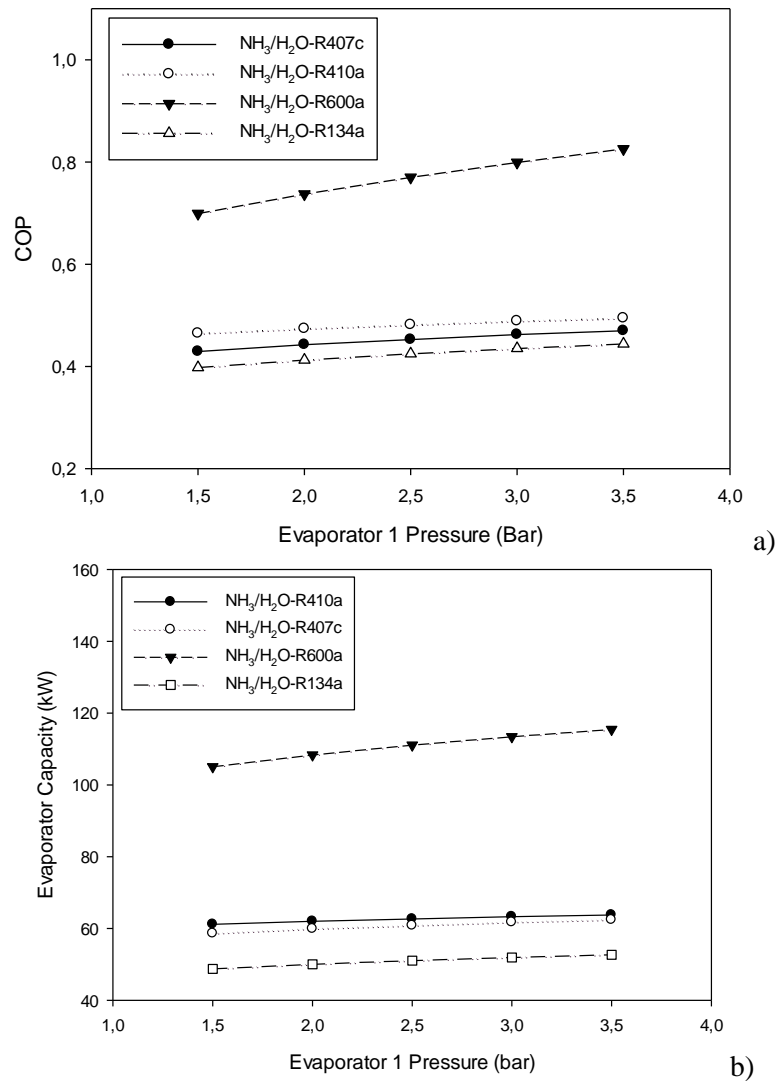
**Figure 13.** Effect of evaporator pressure on a) COP b) Evaporator Capacity
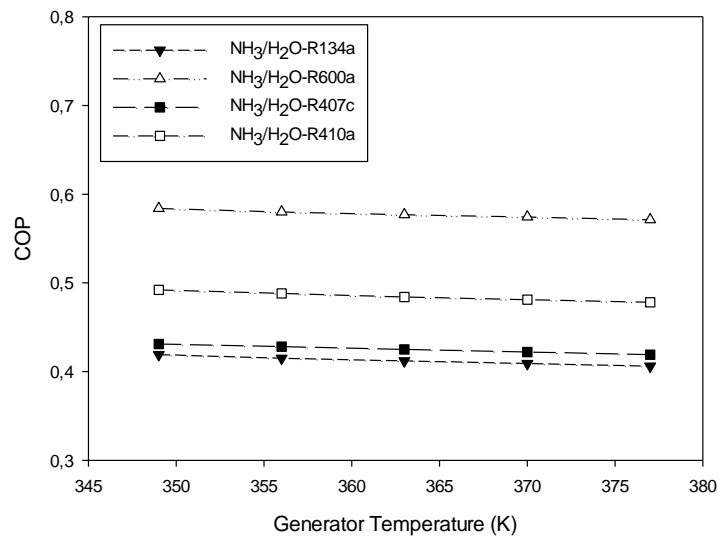
Figure 14. Effects of generator temperature on COP

Figure 12 shows the condenser2 capacity as a function of pressure in the condenser in the absorption section of the cycle. In the calculations, the maximum condenser2 capacity is determined as 61.8 kW using Eq. (4). Condenser2 capacity significantly decreases as pressure in the condenser increases.

The following results are obtained for thermoeconomic analyses.

When considering all calculations, it is clear that using R600a in the VC with NH_3/H_2O VA yields better results than other refrigerants.

Figure 13 shows the COP and Q_{evap}, respectively, as a function of evaporator pressure for various refrigerants used in the VC division. As seen in these figures, the COP and Q_{evap} increase as condenser temperature increases, which is as expected. This increase is more conspicuous when using R600a in the VC division of CS. Increasing the evaporator pressure leads to increased heat capacity of the evaporator for the VC section and decreases compressor power. Using R600a in the VC section of the cycle, the COP and Q_{evap} increase to 0.82 and 115 kW, respectively.

The changes of COP and W_{comp} relative to evaporator temperature are presented in Figure 16 for various refrigerants used in the VC section. As shown in Figure 5, COP increases as evaporator temperature of the cycle increases. When the evaporator temperature and pressure increase, the compression power of the VC section decreases. Therefore, the temperature difference between the cascade heat exchanger and the evaporator decreases, which leads to decreased compressor power and increased COP. Additionally, the refrigerant R600a is observed to have the best performance and the most compressor power in these refrigerants with values of 0.63 and 41.25 kW for COP and W_{comp}, respectively.

Figures 14 and 15 present the COP and Qgen, respectively, as a function of generator temperature for various refrigerants used in the VC division. The COP decreases as the cycle's generator temperature increases. Hence, the maximum COP is obtained at the minimum generator temperature. The highest COP value obtained is 0.58 at 349 K in the generator of the absorption section of the cycle. Moreover, R134a has the poorest performance with 0.41, as shown in Figure 14.

The preliminary comparison of two alternative refrigeration systems, i.e., VC and VC–VA cascaded refrigeration system, is done for different capacities. The other refrigeration system is done for different capacities. The other operating conditions for both the systems are also the same.

The initial cost of the VC system includes a reciprocating chiller, air fan and chilled water pump, whereas initial costs of CS includes cost of VC (including reciprocating chiller, cascade condenser and chilled water pump) and VA systems (including absorption system costs, solar system costs to supply heat in the generator and air fan). Operating cost includes the cost of electricity for running the compressor of both systems. The running costs of auxiliary items, maintenance costs, replacement costs, salvage costs, etc. are not considered in this preliminary study. The economic data for VC and CS systems are given in Table 4.

Using economic analysis, it is observed that even though the initial installation costs for the proposed CS are higher than those of a conventional VC chiller, the shorter payback period makes it commercially. Other refrigerants' payback period are shown in Table 5.

Table 4. The economic data for VC and CS

	R134a		R407c		R410a		R600a	
	VC	CS	VC	CS	VC	CS	VC	CS
Capital Investment Cost ($)	4444	22222	4444	22222	4444	22222	4444	22222
Compressor Power (kW)	6.8	-	22.6	-	15.5	-	47.5	-
Pump Working Load(kW)	-	0.28	-	0.28	-	0.28	-	0.28
Tot. Comp. Power Per Day(kW)	102	4.2	339	4.2	233	4.2	713	4.2
Commercial Electrical Charge Per Unit	0.13	0.13	0.13	0.13	0.13	0.13	0.13	0.13
Total Electric Cost Per Day For Compressor($)	35400	0.53	43.09	0.53	42519	0.53	90.57	0.53
The Cost Electric Charge For Compressor Per Month($)	336.8	13.9	1120.4	13.9	768	13.9	2354.7	13.9
The Annual Electricity Cost For Compressor($)	4042	167	13445	167	9216	167	28257	167
Net Annual Savings	3875.6		13278.6		9049.4		28089.8	

Table 5. Payback periods for different refrigerants

Refrigerant	Payback Period
NH_3/H_2O-R134a	5,7 years
NH_3/H_2O-R600a	0,8 years
NH_3/H_2O-R410a	2,45 years
NH_3/H_2O-R407c	1,7 years

5. CONCLUSIONS

Compression-absorption cascade refrigeration cycle has been analyzed using various refrigerants in the VC section, as have been LiBr/H_2O and NH_3/H_2O fluid pairs in absorption section in terms of the first and second laws of thermodynamics. The performance of refrigerants R134a, R407c, R410a and R600a have been compared under the same conditions. LiBr/H_2O and NH_3/H_2O have been used in the absorption section to compare the refrigerants' effects on system performance.

The results obtained from the energy and exergy analyses are as follows:

a)   Using R600a in the VC section of the cascade cycle leads to a higher efficiency than the other considered refrigerants.

b)   The highest COP and ECOP values are obtained using R600a in the VC section. In contrast, R134a in the VC section is found to be the least efficient refrigerant because it has the lowest COP and ECOP values under constant parameters. The cycle working with LiBr/H$_2$O-R600a has 1.55 times higher COP than the cycle working with LiBr/H$_2$O-R134a for constant evaporator and generator temperatures. The cycle working with LiBr/H$_2$O-R600a has 1.5 times higher ECOP than the cycle working with LiBr/H$_2$O-R134a for constant evaporator and generator temperatures.

c)   Results show that the COP and ECOP values increase as evaporator1 temperature increases, and these values decrease as generator temperature increases using the considered refrigerants in the VC section of the cascade cycle. LiBr/H$_2$O-R600a has the highest value of evaporator capacity, 2 times that of LiBr/H$_2$O-R134a's value. In addition, evaporator capacity increases as evaporator pressure increases.

d)   Generator capacity varies for the different generator temperatures investigated; it is found that this variable increases as generator temperature increases.

e)   The capacity of condenser2 is investigated according to changes in pressure. Results show that the capacity decreases as pressure increases.

   The results obtained from the thermoeconomic analyses are summarized as follows:

a)   Considering the same input temperatures for the evaporator and condenser, R600a has the highest efficiency. Other refrigerants, in descending order of efficiency, are R410a, R407c and R134a.The reason that R600a has the best COP is because R600a has the highest values of enthalpy for the temperatures considered. Given that evaporator capacities are up to enthalpy values, COP is affected in the same way as the capacities.

b)   Using five different generator temperatures, COP is investigated with six different refrigerants, finding that COP decreases as the generator temperature of the CS increases. Thus, it is clear that the most efficient one is R600a. In descending order of efficiency are the following refrigerants: R410a, R407c, R134a. R600a's COP is nearly 1.5 times greater than that of R134a.

c)   If we evaluate the capacities of condenser1, R600a is confirmed to have the highest capacity and R134a the lowest capacity of the six considered refrigerants. R600a has nearly three times more capacity than R134a's.

The calculations included herein show that R600a has the shortest payback period and R134a the longest payback period for the considered refrigerants. In descending order of payback period, the other refrigerants are R407c, R410a. R134a's payback period is nearly six times longer than that of R600a.

NOMENCLATURE

COP   coefficient of performance
CS   cascade system
e   specific exergy [kJ kg-1]
$\dot{E}$ exergy flow rate [kW]
ECOP   exergetic efficiency
f   circulation ratio
ε   effectiveness of the solution heat exchanger
h   enthalpy [kJ kg-1]
$\dot{m}$ mass flow rate [kg s-1]
P   pressure [kPa]
s   specific entropy [kJ kg-1 K -1]

Q̇	heat flow rate [kW]
T	temperature [K]
VA	vapor absorption cooling system
VC	vapor compression cooling system
Ẇ	work flow rate or power of compressor [kW]
x	concentration
NS	annual net saving ratio
PC	power cost [$]

Subscripts

abs	absorber or absorption system
comp	compressor
con	condenser
cyclegen	cycle general
evap	evaporator
gen	generator
i	input
o	output
0	ambient
rev	refrigerant expansion valve
sev	solution expansion valve
she	solution heat exchanger
t	total system

REFERENCES

[1] Cimsit C, Ozturk IT. Buhar sıkıştırmalı-absorbsiyonlu çift kademeli soğutma çevrimi ve alternatif çevrimlerle karşılaştırılması. Isı Bilim Tek Derg 2014; 34(1): 19-26.

[2] Solum C, Heperkan H. Jeotermal enerjili çift etkili lityum bromür – su akışkanlı absorbsiyonlu soğutma sisteminin ekserji analizi. Tesis Müh 2015; 147: 27-34.

[3] Bouaziz N, Benlffa R, Nehdi E, Kairouani L. Conception of an absorption refrigerating system operating at low enthalpy sources. Thermodynamics- Systems in Equilibrium and Nonequilibrium, InTech, 2011.

[4] Cimsit C, Ozturk IT, Hosoz M. Second law based thermodynamic analysis of compression-absorption cascade refrigeration cycles. Isı Bilim Tek Derg 2014; 34(2): 9-18.

[5] Yakar G, Karabacak R, Altan B D. Absorpsiyonlu soğutma sistemleri ile mekanik sıkıştırmalı soğutma sistemlerinin etkinlik ve ekserji verimlilikleri yönünden karşılaştırılmaları. Pamuk Üni Müh Fak Derg 2005; 11(2): 161-169.

[6] Kaynaklı Ö, Yamankaradeniz R. Absorpsiyonlu soğutma sistemlerinde kullanilan eşanjörlerin sistemin performansina etkisi. Ulu Üni Müh Fak Derg 2003; 1: 111-120.

[7] Öcal P, Pıhtılı K. Kademeli soğutma sistemlerinde belirli soğutucu akışkanlar için ikinci kanun analizi. In: 2. Ulusal İklimlendirme Soğutma Eğitimi Sempozyumu ve Sergisi; 23-25 October 2014; Balıkesir, Turkey: pp. 23-25.

[8] Selbas R. Absorbsiyonlu soğutma sistemlerinde absorber sıcaklığının etkisinin termodinamik ve termoekonomik analizi. Süley Demir Üni Fen Bilim Enst Derg 2006; 10-1: 136-143.

[9] Seewald JS, Perez-Blanco H. A simple model for calculating the performance of a lithium-bromide/water coil absorber. Ashrae Transactions 1993; 100(2)-3814: 3814-3824.

[10] Solum C, Koç İ, Altuntaş Y. Çift etkili LiBr/H$_2$O akışkanlı absorpsiyonlu soğutma sisteminde termodinamiksel büyüklüklerin sistem performansina etkileri. Hav Uzay Tekn Derg 2011; January 1(5): 19-26.

[11] Yakut AK, Şencan Ş, Selbaş A, Dikmen R, Görgülü E, Dostuçok Bİ, Kutlu S. Güneş enerjisi destekli absorbsiyonlu soğutma sisteminin termodinamik incelemesi. İKLİM 2011 Ulusal İklimlendirme Kongresi; 18-20 December 2011, Antalya, Turkey: pp. 51-60.

[12] Jain V, Kachhwaha SS, Sachdeva G. NLP model based thermoeconomic optimization of vapor compression-absorption cascaded refrigeration system. Energ Convers Manage 2014; 93: 49-62.

[13] Jain V, Kachhwaha SS, Sachdeva G. Thermodynamic performance analysis of a vapor compression-absorption cascaded refrigeration system. Energ Convers Manage 2013; 75: 685-700.

[14] Karakas A, Egrican N, Uygur S. Second-law analysis of solar absorption-cooling cycles using lithium bromide/water and ammonia/water as working fluids. Appl Energ 1990; 37: 169-187.

[15] Jain V, Kachhwaha SS, Sachdeva G. Energy analysıs of a vapor compressıon system cascaded wıth ammonıa–water absorptıon system. Int J Air-Con Refrig 2014; 22(1), 1450007: 1-12.

[16] Tailor PR, Vipin N. Vapour compression-absorption cascade refrigeration system-thermodynamic analysis. Rec Adv Fl Mech Therm Eng 2014; 12: 127-132.

[17] Kaynaklı Ö, Yamankaradeniz R. Absorpsiyonlu soğutma sistemlerinde kullanilan eşanjörlerin sistemin performansina etkisi. Pamuk Üni Müh Fak Derg 2003; 8(1): 111-120.

[18] Mukhopadhyay N, Chowdhury N. Performance analysis of solar assisted cascade refrigeration system of cold storage system. Int J Adv Res Elect Electro Instr Eng 2013; 2(4): 1248-1254.

[19] Sözen A, Ataer ÖE. Amonyak/su ile çalişan absorbsiyonlu soğutma sistemlerinde isi değiştiricilerin performansa etkisi. 4. Ulusal Tesisat Mühendisliği Kongresi ve Sergisi; 4-7 November 1999; İzmir, Turkey: pp. 403-413.

[20] Talbi MM. Agnew, B. Exergy analysis: An absorption refrigerator using lithium bromide and water as the working fluids. Appl Therm Eng 2000; 20: 619-630.

[21] Jain V, Kachhwaha SS, Sachdeva G. Performance analysis of a vapor compression-absorption cascaded refrigeration system with undersized evaporator and condenser. J Enery South Afric 2014; 25(4): 23-36.